Cardiac MR Imaging with External Respirator: Synchronizing Cardiac and Respiratory Motion—Feasibility Study[1]

Sven Plein, MD
Sudantha Bulugahapitiya, MD
Tim R. Jones, BSc
Gavin J. Bainbridge, BSc
John P. Ridgway, PhD
Mohan U. Sivananthan, MD

Index terms:
Heart, MR, 524.12142, 541.12142, 542.12142
Magnetic resonance (MR), functional imaging, 524.12142, 541.12142, 542.12142
Magnetic resonance (MR), motion correction, 524.12144, 541.12144, 542.12144
Magnetic resonance (MR), vascular studies, 524.12142, 541.12142, 542.12142

Published online before print
10.1148/radiol.2273020148
Radiology 2003; 227:877–882

Abbreviations:
CNR = contrast-to-noise ratio
ECG = electrocardiography
SNR = signal-to-noise ratio

[1] From the Cardiac Magnetic Resonance Unit (S.P., S.B., T.R.J., G.J.B., M.U.S.) and Department of Medical Physics (J.P.R.), General Infirmary at Leeds, Great George St, Rm 170, D-floor, Jubilee Wing, Leeds LS1 3EX, England. Received February 25, 2002; revision requested April 24; final revision received August 29; accepted September 30. S.P. supported by a British Heart Foundation Research Fellowship. **Address correspondence to** S.P. (e-mail: *sven.plein@leedsth.nhs.uk*).

Author contributions:
Guarantor of integrity of entire study, S.P.; study concepts and design, S.P., J.P.R., M.U.S.; literature research, S.P.; clinical studies, S.P., S.B., T.R.J.; data acquisition, T.R.J.; data analysis/interpretation, S.P., S.B., G.J.B.; statistical analysis, S.P.; manuscript preparation, S.P., J.P.R., T.R.J., S.B., M.U.S.; manuscript definition of intellectual content and editing, S.P.; manuscript revision/review and final version approval, all authors.

The feasibility of electrocardiography (ECG)-synchronized respiration with an external cuirass-type respirator in cardiac magnetic resonance (MR) imaging was evaluated. Cardiac MR imaging was performed in 10 nonsedated healthy volunteers with an ECG-triggered external respirator that was modified for use in the MR environment. Coronary MR angiograms and multiphase gradient-echo cine images were acquired with one respiratory cycle performed per cardiac cycle. The technique was feasible and in this group of volunteers resulted in equivalent image quality but shorter acquisition times than those of conventional free-breathing and breath-holding techniques.

The motion of the heart in the cardiac and respiratory cycles is a major impediment to cardiac magnetic resonance (MR) imaging. In standard data acquisition methods that use multiple heartbeats, compensation methods for this motion must be used. The effect of cardiac motion is accounted for by synchronizing the image acquisition to electrocardiography (ECG) or to the peripheral pulse (1–8). The effect of respiratory motion is most commonly minimized by breath holding (1–3) or accounted for by navigator-based respiratory gating methods (4–8). As respiration and cardiac motion are asynchronous events, conventional methods of compensation are also performed separately, and data acquisition is thus limited to the time when both cardiac and respiratory compensation coincide. This can result in low imaging efficiencies of data acquisition in cardiac MR imaging.

External cuirass-type respirators allow noninvasive regulation of the respiration of nonsedated subjects. They can generate highly reproducible chest wall and diaphragmatic excursions (9,10) and can be triggered by ECG. If the devices are set to perform one respiratory cycle per R-R interval, identical respiratory movements can be generated in every cardiac cycle. When applied to cardiac MR imaging, this may permit a synchronized approach to cardiac and respiratory motion compensation, as data could be acquired in every cardiac cycle without the need for breath holding or respiratory navigator gating. Thus, the efficiency of image acquisition may be improved and imaging times may be shortened.

In this study, we evaluated the feasibility of ECG-synchronized respiration with an external respirator in cardiac MR imaging.

Materials and Methods

Study Population

The study population comprised 10 healthy volunteers (seven men, three women; mean age, 25 years; range, 21–36 years) without prior experience with MR imaging or the external respirator. Volunteers had no history of cardiac or other illness and had normal resting ECG findings, normal blood pressure, and normal physical examination results. Their mean body weight was 79.7 kg (range, 65–99 kg) with a mean body mass index of 24.8 (range, 21.1–30.1). Written informed consent was obtained from all subjects. Subjects with contraindications to MR imaging, arrhythmia, respiratory disease, or chest wall deformities were not re-

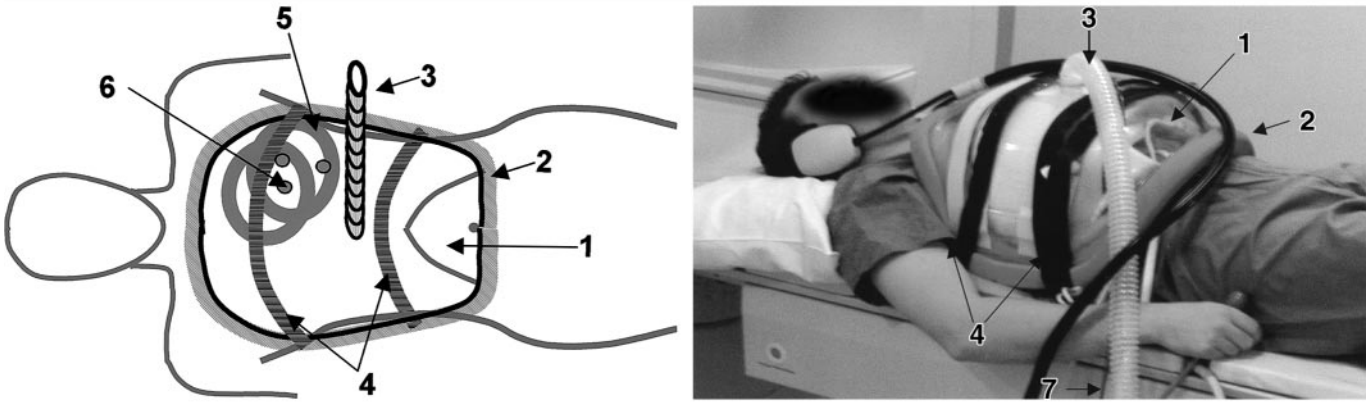

a. b.

Figure 1. Setup of external respirator for MR imaging. **(a)** Schematic setup. **(b)** Setup with a volunteer. *1* = cuirass, *2* = foam seal, *3* = flexible tubing, *4* = hook and loop straps, *5* = cardiac receiver coil, *6* = ECG electrodes, *7* = pressure transducer.

cruited. The study protocol was approved by the local ethics review committee, and written informed consent was obtained from all recruited subjects.

The Respirator

The external respirator used in this study (RTX; Medivent, London, England) consists of a portable computerized power and control unit, which is attached by a flexible large-bore tube to a cuirass (Fig 1). The cuirass is made of specially formulated and molded clear plastic. It fits over the front of the chest and abdomen to include the umbilicus. The sides of the cuirass are bordered with soft foam rubber to provide a comfortable airtight seal. The standard cuirass was custom-modified for use in the MR environment in this study. The modified cuirass extends mainly anteriorly to contain the cardiac receiver coil and fits closely to the sides of the subject. The power unit generates a cyclic pressure change inside the cuirass, with positive pressure creating inspiration and negative pressure creating expiration. A pressure transducer connected to the inside of the cuirass transmits pressure data to the control unit so that exact pressures and thus diaphragmatic and chest wall positions can be generated and maintained. Both inspiratory and expiratory phases are actively controlled, ensuring that the respiratory positions between repeated cycles are highly reproducible. Pressures up to plus or minus 70 cm H_2O and respiratory rates of 1–1,000 cycles per minute can be generated. For this study, the control unit was programmed so that in the ECG-triggered mode ventilation was synchronized to the R wave. The duration and depth of expiration and inspiration and the delay of the respiratory phases from the R wave could be freely chosen. The device can be set to trigger a respiratory cycle at every cardiac cycle or at other ratios. In this study, the external respirator was used in the ECG-triggered mode for all imaging, with a 1:1 ratio of respiratory and cardiac cycles.

Setup and Preparation

ECG leads were placed on the anterior or posterior chest wall of the subjects, with care taken to generate an optimal ECG signal. We used a monitoring system (model MR9500; Medrad, Indianola, Pa) to perform ECG. The main monitoring unit was in the magnet room, with a slave monitor in the control room. A five-element phased-array cardiac synergy coil was placed over the chest wall, and the plastic cuirass was placed over the coil. The cuirass was strapped to the subjects with adjustable hook and loop straps. The control unit of the external respirator was placed outside the magnet room, with the pressure tubes fed into the room through wave guides. For this study, the power unit was modified to take account of the "dead space" created by the extended tubing in the MR imaging setup. The ECG signal detected by the monitoring system was used to trigger both the MR imager and the external respirator simultaneously.

The exact settings of the respirator varied for each subject and were optimized individually according to heart rate and required depth of respiration. Expiratory pressures ranged from 10 to 15 cm H_2O and inspiratory pressures from −10 to −15 cm H_2O, as required to achieve sufficient ventilation (ie, to suppress any spontaneous respiration).

The subjects were familiarized with assisted respiration by operating the device outside the magnet bore prior to commencement of imaging.

Acquisition Protocol

MR imaging was performed with a 1.5-T commercially available system (Gyroscan ACS NT; Philips Medical Systems, Best, the Netherlands) equipped with PowerTrak 6000 gradients (23 mT/m, 105 mT/m/msec) and a five-element cardiac phased-array coil.

Representing the two most commonly used respiratory compensation methods, breath-hold multisection multiphase gradient-echo MR images of the left ventricle and respiratory navigator–gated images of the coronary arteries were acquired. Acquisitions were performed in random order both in the conventional fashion while the external respirator was switched off and during synchronized respiration with the device switched on.

All subjects underwent coronary MR angiography of both the left and right coronary arteries. Data acquisition was performed with a three-dimensional segmented k-space gradient-echo sequence, as described by Botnar et al (8) (7/2.1 [repetition time msec/echo time msec]; flip angle, 25°; T2 preparation prepulses; field of view, 400 × 300 mm; matrix, 512 × 384; in-plane spatial resolution, 1.04 × 0.78 mm; 10 contiguous 3-mm-thick sections interpolated during reconstruction to 20 1.5-mm-thick sections). For conventional imaging, data were acquired during free breathing with prospective navigator gating with real-time correction of the three-dimensional volume position in the craniocaudal direction. For respirator-triggered acquisition, data were acquired with the respirator

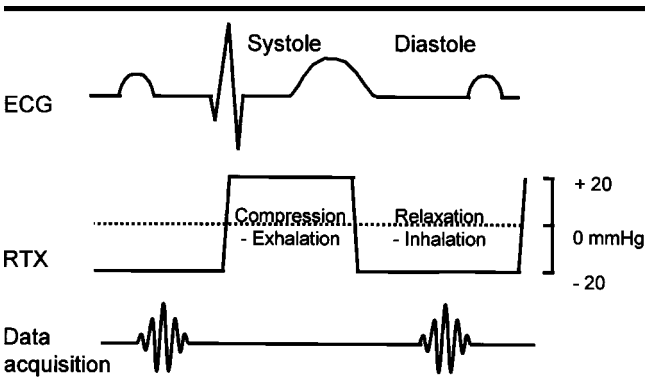

Figure 2. Schematic representation of synchronized data acquisition at coronary MR angiography with use of the external respirator *(RTX)*. The respirator is set to generate a short end-expiratory phase in early systole and a slow inspiratory phase in diastole. Data are acquired in diastole, when both the coronary motion in the cardiac cycle and the respiratory motion are minimal.

generating one respiratory cycle in every R-R interval. The respiratory trigger delay and expiratory duration were selected to ensure minimal chest wall and diaphragmatic motion during the acquisition phase in mid-diastole (Fig 2). The delay of the respiratory cycles from the R wave at ECG was set to between 80% and 100% of the R-R interval for coronary MR angiography. The expiratory duration was set to 260–300 msec (mean, 275 msec), with inspiration set to occur in the remaining R-R interval. During data acquisition, a respiratory navigator was also applied to allow an assessment of the reproducibility of the respiratory movements.

In nine subjects, multiphase cine data sets of the left ventricle were acquired with a conventional cine gradient-echo sequence in short-axis orientation (segmented k-space turbo gradient echo: 8.8/5.2; flip angle, 35°; one signal acquired; spatial resolution, 1.33 × 2.65 mm; 6-mm section thickness; 4-mm intersection gap; 10–15 phases per cardiac cycle; 10–14 sections to cover the left ventricle). In one subject, gradient-echo cine images could not be acquired because of time constraints. Conventional images (without the external respirator) were acquired in breath holds of 12–16 seconds duration per section. With the external respirator in operation, the sections were acquired sequentially and continually with no pause between each section acquisition. The delay of the respiratory cycles from the R wave at ECG was set to 100% (no delay) for gradient-echo cine images.

To assess subject tolerance of the external respirator, they were asked by one of the investigators (S.P. or S.B.) if the device caused any pain or discomfort either at rest or during assisted respiration. Any such effects were documented. All subjects were also asked if they regarded the device as "tolerable" in the magnet bore.

Image Analysis

The imaging time and (for coronary imaging) the navigator efficiencies were recorded by one of the investigators (S.P. or S.B.). For coronary imaging, the acquisition time excluded the navigator preparation and data reconstruction times. For gradient-echo cine imaging without the respirator operating, time was recorded from the start of the instructions for the first breath hold until completion of the last breath hold. For acquisition with the respirator operating, the total time for acquisition of all sections was measured.

Images were transferred to a standalone workstation (EasyVision; Philips Medical Systems) and analyzed independently and in random order by two experienced observers (S.P., S.B.), who were blinded to the acquisition type.

The multiphase cine images were analyzed by consensus of the two observers for overall image quality on a scale of 0–4: 0, not interpretable; 1, poor (substantial image artifacts or poor definition of the cardiac structures); 2, average (minimal artifacts but all major cardiac structures identifiable); 3, good (no artifacts and all cardiac structures clearly demarcated); and 4, excellent (outstanding delineation of all cardiac structures). One observer (S.P.) then placed standard-sized regions of interest (100 mm^2) in both the blood pool and the myocardium. The mean signal intensity (SI) and the SD of the signal intensity in these regions of interest were measured. From these measurements, the signal-to-noise ratios (SNRs) of blood pool and myocardium and the blood-myocardial contrast-to-noise ratio (CNR) were calculated as follows: SNR = Mean SI/SD; CNR = $(SI_{blood} - SI_{myocardium})/[½(SD_{blood} + SD_{myocardium})]$.

For analysis of coronary arteries, image quality was scored by consensus of both observers on a five-point scale: 0, vessel not seen; 1, poor (substantial image artifacts or vessels poorly defined); 2, average (minimal artifacts but vessels easily identifiable); 3, good (no artifacts and vessels clearly demarcated); and 4, excellent (outstanding definition of coronary vessels). The visible length of the combined left main and left anterior descending coronary arteries and of the right coronary arteries was measured by one observer (S.P.) from the outer edge of their respective aortic sinuses on multiplanar reformations. As for the analysis of cine images, one observer (S.P.) placed standard-sized regions of interest (100 mm^2) in the blood pool and the myocardium, and the SNR of the blood pool and the CNR between blood pool and myocardium were calculated.

All data are presented as mean plus or minus SD. Formal statistical analysis was not carried out in view of the small sample size of our study population in this initial feasibility study.

Results

MR imaging proved feasible with the external respirator in all subjects and for the applications tested. The external respirator achieved synchronization of respiration to the cardiac cycle in all subjects. All subjects tolerated the assisted respiration well, and familiarization took less than 5 minutes in all instances. All 10 subjects regarded this external respirator device as "tolerable." No subject experienced pain from the device. Two subjects experienced transient paraesthesia in the hands caused by pressure from the edge of the cuirass in the axilla, which necessitated repositioning of the cuirass.

In three volunteers, considerable artifacts were induced by the moving cuirass superimposed on the T wave at ECG. This was improved sufficiently to allow data acquisition by placing the ECG leads on the backs of the individuals at a position remote from the anterior chest wall motion. However, in two subjects, ECG artifacts remained and caused intermittent loss of synchronization of the respirator

with ECG during acquisition of gradient-echo cine images.

Gradient-Echo Cine Imaging

The total acquisition time at gradient-echo cine imaging was shorter with respirator-triggered acquisition than with conventional breath-hold acquisition (Table 1). The mean image quality score was slightly lower for respirator-triggered than for conventional acquisition. The differences in image quality were caused by motion artifacts on the two respirator-triggered data sets, in which there was intermittent misregistration at ECG. These data sets received a lower quality score than that of the corresponding conventional images. SNR and CNR measurements were similar between the two methods (Table 1). Figure 3 shows end-diastolic and end-systolic images acquired during respirator-controlled respiration; they demonstrate comparable image quality. The figure also shows the different chest positions in diastole and systole that were induced by the respirator.

TABLE 1
Gradient-Echo Cine Imaging of the Left Ventricular Volume: Comparison of Conventional and Respirator-triggered Acquisitions

Technique	Imaging Time (min:sec)	Image Quality Score	SNR		Blood-Muscle CNR
			Blood	Muscle	
Conventional	3:30 (0:25)	3.4 (0.8)	16.1 (5.7)	7.5 (3.1)	10.1 (3.8)
Respirator triggered	2:21 (0:18)	2.8 (0.8)	15.2 (6.9)	7.2 (2.8)	9.8 (3.3)

Note.—Unless indicated otherwise, data are the mean, and numbers in parentheses are the SD.

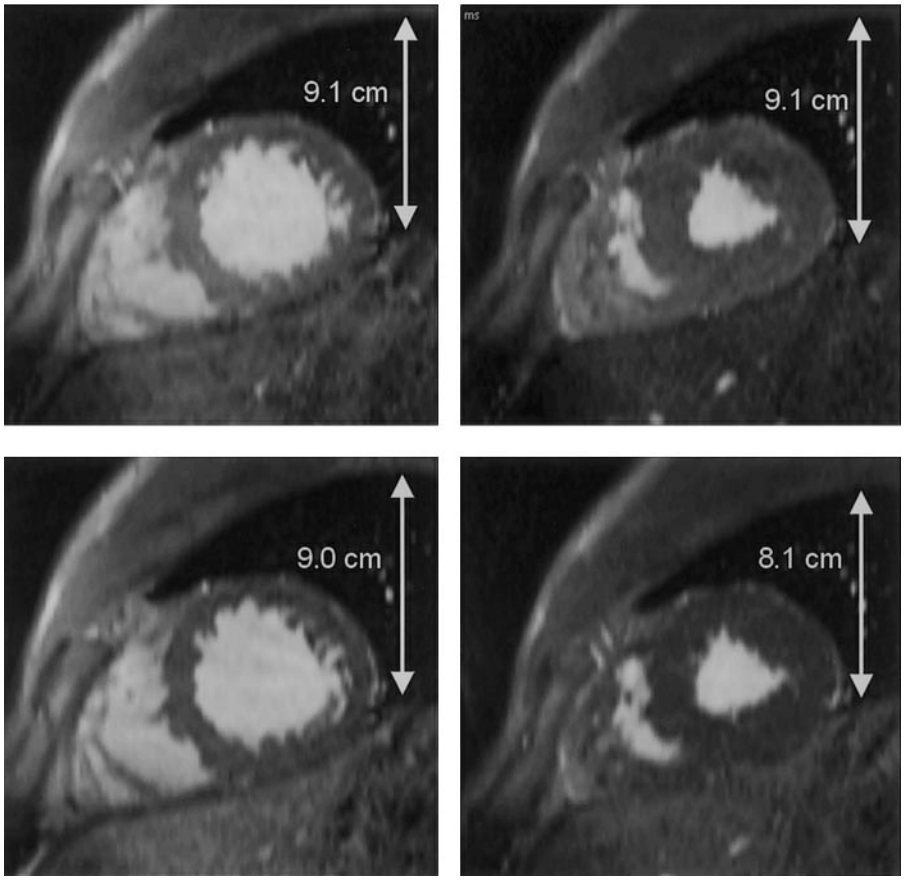

Figure 3. Images from a multiphase data set. Left: End-diastolic images. Right: End-systolic images. Top: Conventional acquisitions. Bottom: Respirator-triggered acquisitions. Images obtained in both acquisitions were scored as having good image quality, and objective measurements showed no substantial differences. Arrows indicate the distance between chest wall and diaphragm. In the conventional images, this distance remains unchanged between diastole and systole. In the respirator-triggered images, the distance is shorter in systole, which reflects chest compression in inspiration.

Coronary MR Angiography

Acquisition with respirator-controlled respiration resulted in reductions in the acquisition times and a twofold improvement in navigator efficiencies compared with those with conventional acquisition (Table 2). On no occasion was the acquisition time or the navigator efficiency worse with the use of the respirator. The image quality scores were comparable between the two techniques. Examples of a right coronary artery angiogram acquired with and one acquired without use of the external respirator are given in Figure 4. Objective measurements of coronary vessel length, CNR, and SNR were also similar (Table 2).

Discussion

Current Respiratory Compensation Techniques

Currently methods of cardiac and respiratory motion compensation in cardiac MR imaging result in relatively low efficiency of data acquisition. In particular, the respiratory compensation techniques have limitations in clinical practice. Breath holding requires substantial cooperation by patients and depends on their breath-holding capabilities. The end-expiratory position can show considerable variability between repeated breath holds even in healthy volunteers. The limited duration of a breath hold is an important constraint for complex imaging procedures such as coronary artery imaging. Modified breath-hold techniques, such as multiple short breath holds (11) and respiratory feedback monitoring (12–14), have not gained wider acceptance because of even greater dependence on patient cooperation. In non–breath-hold (free-breathing) techniques, respiratory gating is used either with external respiratory bellow monitoring (15) or with navigator echoes (5–8), which track and adjust for the diaphragmatic or cardiac position. These techniques are useful with longer more complex imaging sequences, such as high-spatial-resolution three-dimensional acquisitions, but they also have a number of limitations. Imaging efficiency is relatively low because acquisition is limited to the heart phases within a fixed win-

TABLE 2
Coronary MR Angiography: Comparison of Conventional and Respirator-triggered Acquisitions

Technique	Imaging Time (min:sec)	Navigator Efficiency (%)	Image Quality Score	Vessel Length (mm)	Blood SNR	Blood-Muscle CNR
Left coronary system*						
Conventional	13:43 (5:2)	54 (15.2)	2.1 (0.7)	54 (15.3)	11.4 (2.6)	7.9 (1.6)
Respirator triggered	7:04 (1:2)	96 (7.1)	2.6 (0.5)	55 (18.6)	11.2 (3.6)	7.6 (1.8)
Right coronary system						
Conventional	12:40 (3:2)	49 (14.5)	2.4 (0.5)	84 (19.0)	11.8 (1.9)	8.9 (3.7)
Respirator triggered	8:22 (2:3)	89 (16.6)	2.6 (0.5)	94 (22.1)	12.9 (3.1)	9.3 (2.9)

Note.—Unless indicated otherwise, data are the mean, and numbers in parentheses are the SD.
* Measurements of vessel length are for the combined left main coronary and left anterior descending arteries.

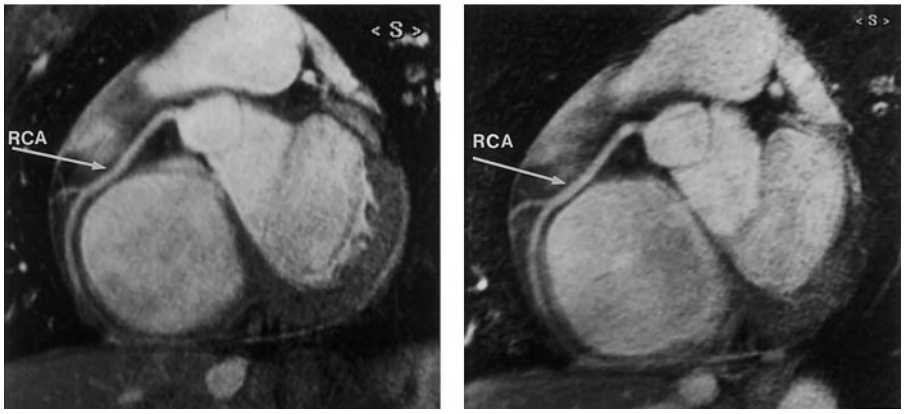

Figure 4. Double-oblique MR angiograms show single sections of the right coronary artery (*RCA*). Left: Image acquired conventionally without the use of the external respirator. Right: Image acquired with the external respirator switched on. Total imaging time for the respirator-triggered acquisition was 45% of that for the conventional acquisition. Navigator efficiency was 95% with the respirator. Both images were scored as 2 (good).

dow of the respiratory cycle, usually end expiration. Therefore, even in healthy and cooperative subjects, imaging efficiency during free-breathing navigator-echo MR imaging is generally in the range of 40%–60% and is often lower (16). Furthermore, drifting of the mean end-expiratory position can occur during long acquisitions, which reduces imaging efficiencies even more. Also, considerable individual variability exists in the relationship between coronary and diaphragmatic respiratory motion during free breathing (17). This complicates the use of predefined correction factors to relate coronary and diaphragmatic positions in navigator-gated data acquisition.

Synchronized Respiration

The external respirator is presently used mainly for the treatment of acute respiratory failure or for respiratory management after cardiac surgery (18–25). In this study, the external respirator was used for an integrated approach to respiratory and cardiac motion correction in cardiac MR imaging. With the device, precise and reproducible synchronization of the respiratory cycle to the cardiac cycle was achieved in the MR environment in a group of volunteers. Imaging sequences that normally require navigator-gated or breath-hold techniques were performed with continuous acquisition during synchronized respiration. The external respirator was well tolerated by this group of subjects, who had no prior experience with the device or with MR imaging, and the learning phase with the device was short.

In this small number of subjects, imaging times were lower and imaging efficiencies were higher with synchronized respiration than those with conventional imaging. Time savings were most substantial in navigator-gated acquisitions, in which imaging times were halved because of higher navigator efficiencies. These efficiencies indicated that the respiratory excursions in each cardiac cycle that were induced by the external respirator were highly reproducible. In breath-hold imaging, the respirator technique reduced imaging times by removing the time conventionally taken for breathing between breath holds. Subjective and objective measurements of image quality were comparable between the two acquisition types. This finding suggests that in gradient-echo cine imaging, the chest motion induced by the external respirator does not affect image quality because the motion occurs reproducibly in each cardiac cycle. For coronary MR angiography, we set the external respirator to generate a relatively slow inspiratory phase during data acquisition in diastole. The finding of image quality that was similar to that with conventional technique suggests that the respirator-induced motion during data acquisition was minimal.

Potential applications of cardiac-respiratory motion synchronization in cardiac MR imaging could be substantial. Results in this study seem to indicate that this technique may remove the time constraints of breath holding and overcome the limited efficiency of navigator imaging, which may allow more efficient and faster image acquisition. The technique is independent of the acquisition sequence used; thus, it can be combined with all MR imaging methods available. The technique should be particularly useful in coronary MR angiography and could be used to increase the resolution of coronary artery imaging or to shorten imaging times in long acquisition protocols.

Patients who are unable to hold their breath might benefit from the device. The external respirator allows adjustment of the depth of respiration to each subject's requirements, and patients with dyspnea could receive mild hyperventilation to improve their comfort in the supine position in the MR imager. Continuous monitoring of P_{O_2} and P_{CO_2} is possible to ensure adequate ventilation. Depending on the timing of the respiratory phases relative to the cardiac cycle, chest compression during expiration may also support systolic contraction, and the negative external pressure during inspiration could increase venous return in diastole. These effects will have to be evaluated in future studies.

Limitations

The main problems encountered in this feasibility study were related to ECG artifacts associated with the use of the

external respirator in the magnetic field. The respirator causes relatively large chest excursions, and in some subjects, this caused ECG artifacts, which in turn caused misregistration by the respirator. The ECG artifacts could be largely avoided by ensuring minimal movements of the ECG leads during respiration and in some cases by placing them on the subject's back. In two volunteers, however, some artifacts remained even when there was no obvious movement of the ECG leads, which affected the quality of the data acquired. These artifacts are probably related to fast movements of blood or chest wall during respiration with the external respirator. The exact effects of the respirator on blood flow will have to be assessed in future work.

Although this external respirator was generally well tolerated, two volunteers had transient paraesthesia in the hands caused by pressure from the cuirass in the axilla. The cuirass that was used for this initial study has since been optimized further to provide more space in the axilla and anteriorly to accommodate the receiver coil. Despite these modifications, the space taken up by the cuirass will inevitably limit its applicability to larger subjects in the confinement of the bore of an MR imager. The largest subject included in this pilot study weighed 99 kg and had a body mass index of 30.2. It may not be feasible to use the external respirator in the MR environment in subjects who exceed this size.

Another limitation of this pilot work is that only young healthy volunteers were studied. The extent to which our results can be reproduced in patients will have to be determined in future work.

In conclusion, synchronization of respiration to the cardiac cycle with the external respirator in cardiac MR imaging was feasible in this initial study, and the results seem to indicate improved imaging efficiency with similar image quality in comparison with conventional free-breathing and breath-holding techniques. Further investigation of this technique in a larger cohort and in patients is required. Potential applications may include use in routine imaging to reduce imaging times or increase image resolution and in imaging in patients with poor breath-holding ability.

Acknowledgments: We thank Zamir Hayek, MD, from Medivent, and Ian Benton from Medrad.

References

1. Sakuma H, Fujita N, Foo TKF, et al. Evaluation of left ventricular volume and mass with breath-hold cine MR imaging. Radiology 1993; 188:377–380.
2. Edelman RR, Manning WJ, Burstein D, Paulin S. Coronary arteries: breath-hold MR angiography. Radiology 1991; 181:641–643.
3. Pennell DJ, Keegan J, Firmin DN, Gatehouse PD, Underwood SR, Longmore DB. Magnetic resonance imaging of coronary arteries: technique and preliminary results. Br Heart J 1993; 70:315–326.
4. Wang Y, Rossman PJ, Grimm RC, Riederer SJ, Ehman RL. Navigator-echo-based real-time respiratory gating and triggering for reduction of respiration effects in three-dimensional coronary MR angiography. Radiology 1996; 198:55–60.
5. Li D, Kaushikkar S, Haacke EM, et al. Coronary arteries: three-dimensional MR imaging with retrospective respiratory gating. Radiology 1996; 201:857–863.
6. Danias PG, McConnell MV, Khasgiwala VC, Chuang ML, Edelman RR, Manning WJ. Prospective navigator correction of image position for coronary MR angiography. Radiology 1997; 203:733–736.
7. Stuber M, Botnar RM, Danias PG, Kissinger KV, Manning WJ. Submillimeter 3D coronary MRA using real-time navigator correction: comparison of navigator locations. Radiology 1999; 212:579–587.
8. Botnar RM, Stuber M, Danias PG, Kissinger KV, Manning WJ. Improved coronary artery definition with T2-weighted, free-breathing, three-dimensional coronary MRA. Circulation 1999; 99:3139–3148.
9. Petros AJ, Fernando SS, Shenoy VS, al-Saady NM. The Hayek oscillator: nomograms for tidal volume and minute ventilation using external high frequency oscillation. Anaesthesia 1995; 50:601–606.
10. Hayek Z, Sohar E. External high frequency oscillation: concept and practice. Intensive Care World 1993; 10:36–40.
11. Doyle M, Scheidegger MB, de Graf RG, Vermeulen J, Pohost GM. Coronary artery imaging in multiple 1-sec breath-holds. Magn Reson Imaging 1993; 1:3–6.
12. Wang Y, Grimm RC, Rossman PJ, Debbins JP, Riederer SJ, Ehman RL. 3D coronary MR angiography in multiple breath-holds using a respiratory feedback monitor. Magn Reson Med 1995; 34:11–16.
13. Liu YL, Riederer SJ, Rossman PJ, Grimm RC, Debbins JP, Ehmann RL. A monitoring, feedback, and triggering system for reproducible breath-hold MR imaging. Magn Reson Med 1993; 30:507–511.
14. Wang Y, Christy PS, Korosec FR, et al. Coronary MRI with a respiratory feedback monitor: the 2D imaging case. Magn Reson Med 1995; 33:116–121.
15. Hundley WG, Clarke GD, Landau C, et al. Noninvasive determination of infarct artery patency by cine magnetic resonance angiography. Circulation 1995; 91:1347–1353.
16. Stuber M, Botnar R, Danias PG, et al. Double-oblique free-breathing high resolution three-dimensional coronary magnetic resonance angiography. J Am Coll Cardiol 1999; 34:524–531.
17. Danias PG, Stuber M, Botnar RM, Kissinger KV, Edelman RR, Manning WJ. Relationship between motion of coronary arteries and diaphragm during free breathing: lessons from real-time MR imaging. AJR Am J Roentgenol 1999; 172:1061–1065.
18. Sideno B, Vaage J. Ventilation by external high-frequency oscillations improves cardiac function after coronary artery bypass grafting. Eur J Cardiothorac Surg 1997; 11:248–257.
19. al-Saady NM, Fernando SS, Petros AJ, Cummin AR, Sidhu VS, Bennett ED. External high frequency oscillation in normal subjects and in patients with acute respiratory failure. Anaesthesia 1995; 50:1031–1035.
20. Gaitini L, Vaida S, Krimerman S, et al. External high-frequency ventilation in patients with respiratory failure (letter). Intensive Care Med 1995; 21:191.
21. Spitzer SA, Fink G, Mittelman M. External high-frequency ventilation in severe chronic obstructive pulmonary disease. Chest 1993; 104:1698–1701.
22. Shekerdemian LS, Schulze-Neick I, Redington AN, Bush A, Penny DJ. Negative pressure ventilation as haemodynamic rescue following surgery for congenital heart disease. Intensive Care Med 2000; 26:93–96.
23. Shekerdemian LS, Bush A, Shore DF, Lincoln C, Redington AN. Cardiopulmonary interactions after Fontan operations: augmentation of cardiac output using negative pressure ventilation. Circulation 1997; 96:3934–3942.
24. Shekerdemian LS, Shore DF, Lincoln C, Bush A, Redington AN. Negative-pressure ventilation improves cardiac output after right heart surgery. Circulation 1996; 94(suppl 9):II 49–55.
25. Shekerdemian LS, Bush A, Shore DF, Lincoln C, Redington AN. Cardiorespiratory responses to negative pressure ventilation after tetralogy of Fallot repair: a hemodynamic tool for patients with a low-output state. J Am Coll Cardiol 1999; 33:549–555.